MetOp-A and MatOp-B AVHRR visible and near-IR channel inter-comparison with BRDF consideration.

Tiejun Chang [1], Fred Wu [2], and Fuzhong Weng [2]

[1] ERT Inc., 6100 Frost Place, Suite A, Laurel, MD 20707, USA
[2] NOAA/NESDIS/STAR, College Park, MD 20740, USA

GSICS Meeting, March, 4, 2013

Acknowledgements
Thanks Wei Guo and Felix Kogan for their contribution.

MetOp-A and MatOp-B AVHRR visible and near-IR channel inter-comparison with BRDF consideration.

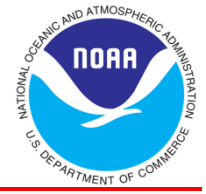

- Introduction
- MetOp-A and MetOP-B inter-comparison
- BRDF effect and modeling
- Libyan Desert reflectance seasonal oscillation
- MetOp-B seasonal oscillation curve regression
- MatOp-B visible and near-IR channel calibration update
- Summary

MetOp-B

MetOp-B: Launched September 17, 2012

Dual MetOp Constellation

- ❑ Same Orbital Track
- ❑ Separated by ½ Orbit (180 degrees)
- ❑ Orbital Sensing difference ~50 mins
- ❑ One is Primary and the other is Secondary

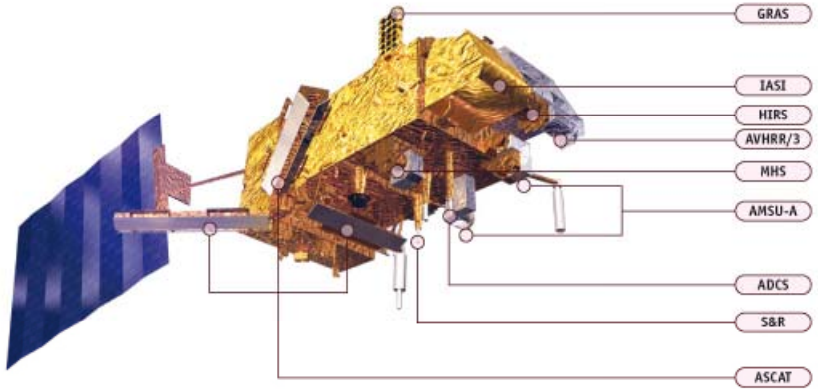

AVHRR

Scan Rate	6 Hz (0.1667 secs)
Scan Type	Continuous scan
Pixel IFOV (3dB beamwidth)	0.0745° (square)
IFOV size at Nadir	1.1 km
Sampling at Nadir	0.87 km
Earth View Pixels / Scan	2048
Swath	± 55.37°
Swath	± 1464 km
Spectral Range	0.6 to 12 µm

MetOp-A and MetOp-B AVHRR inter-comparison

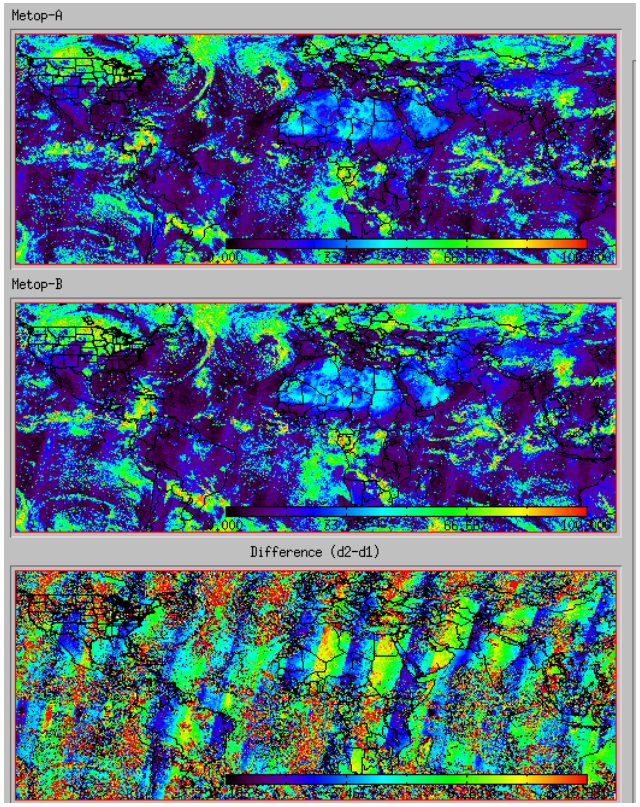

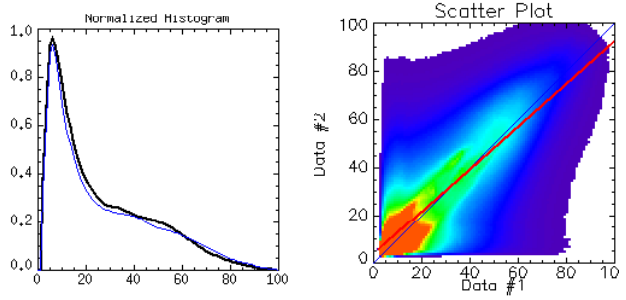

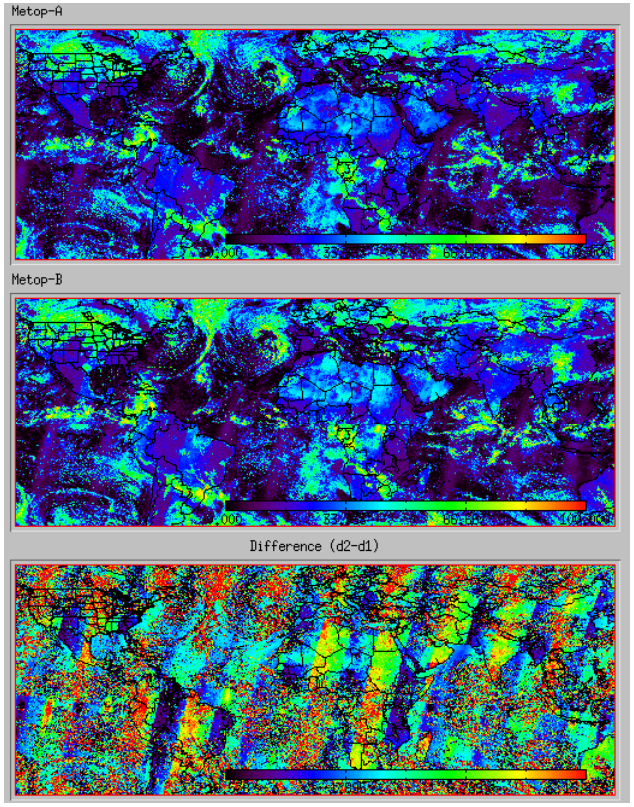

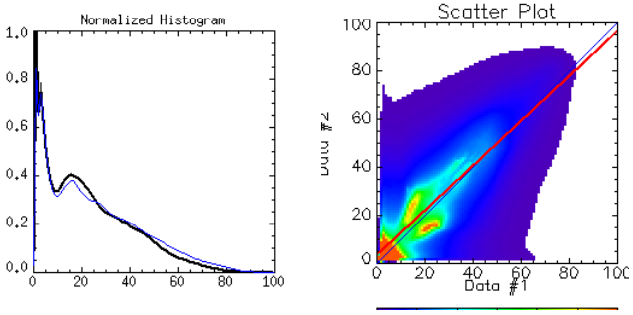

Libyan Desert for inter-comparison and vicarious calibration

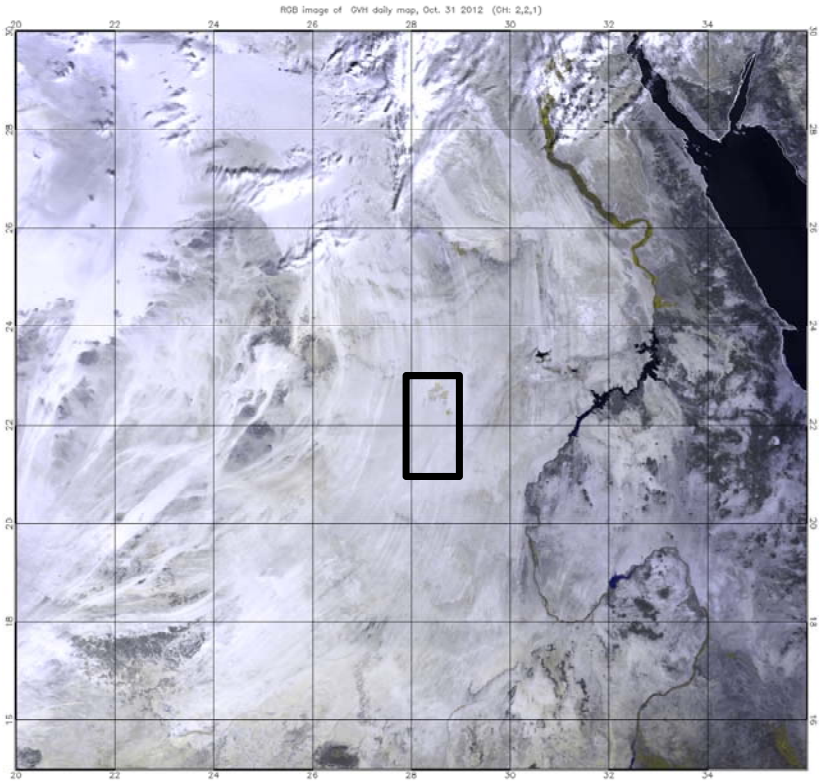

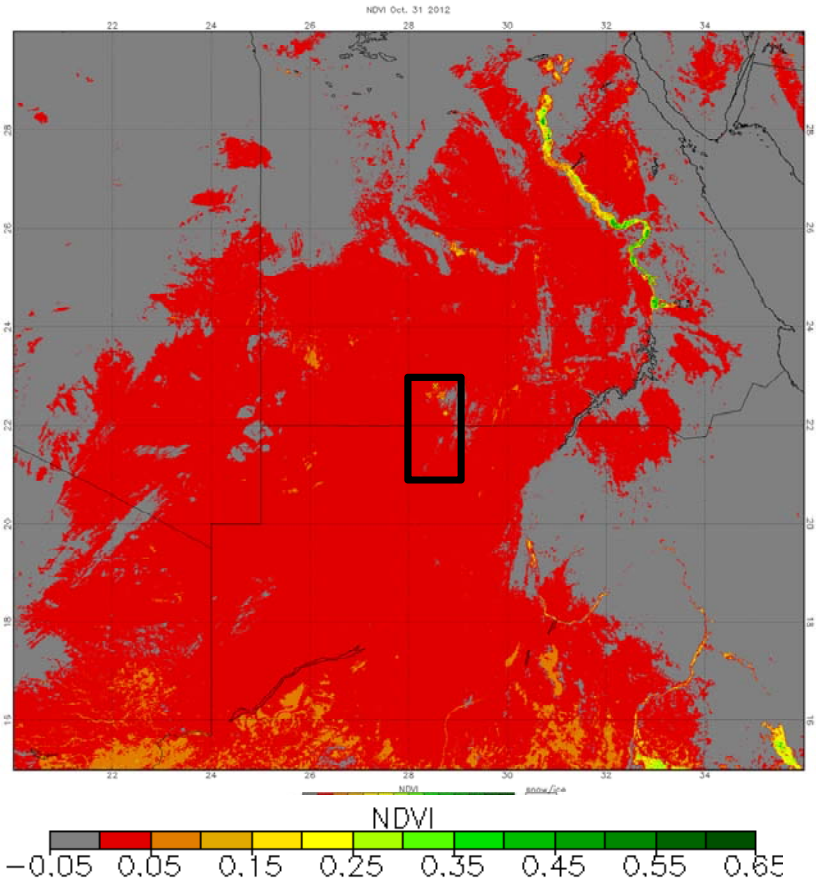

Location of Libyan Desert for AVHRR visible channel calibration

MetOp-B AVHRR images

MetOp-A and MetOp-B inter-comparison at Libyan Desert

Ch 1

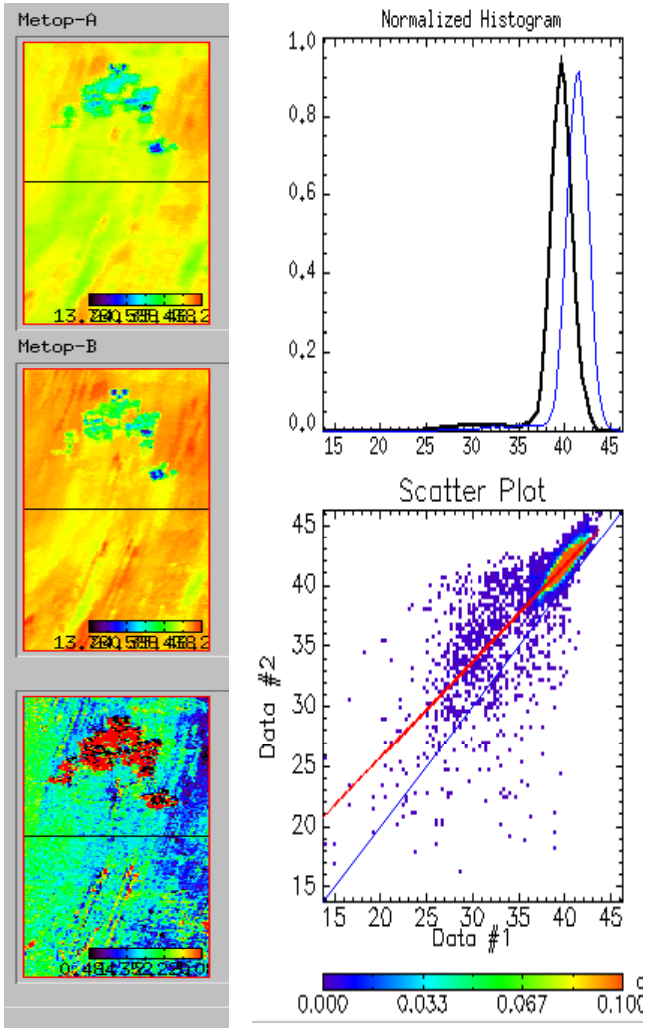

Ch 2

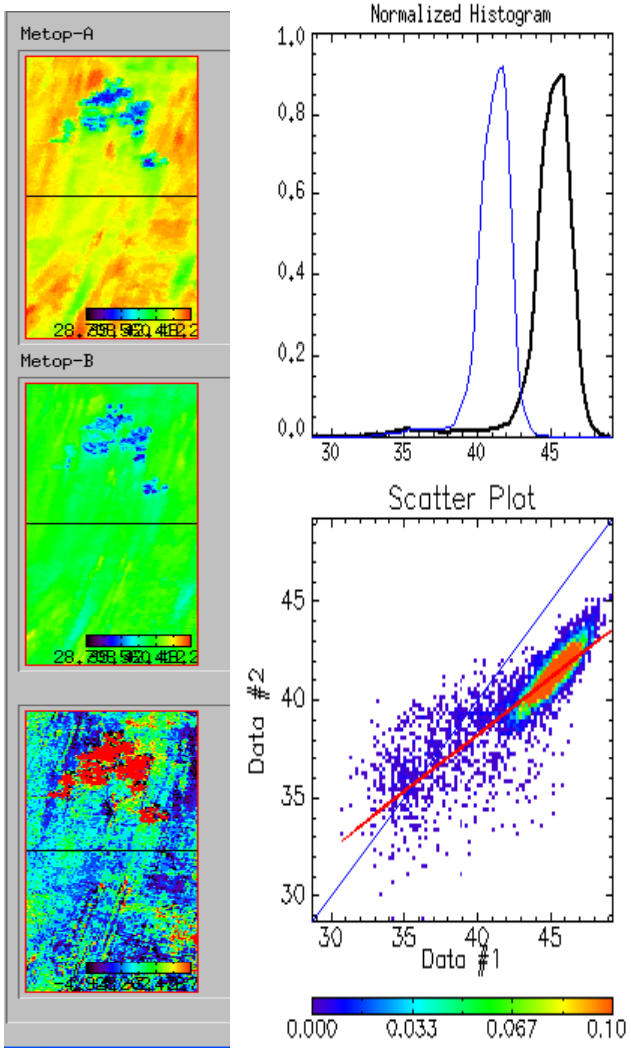

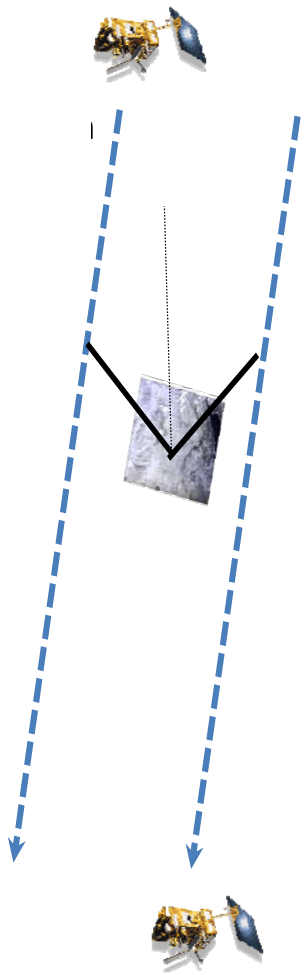

Different instrument zenith angle and Solar zenith angle

MetOp-A and MetOp-B inter-comparison at Libyan Desert

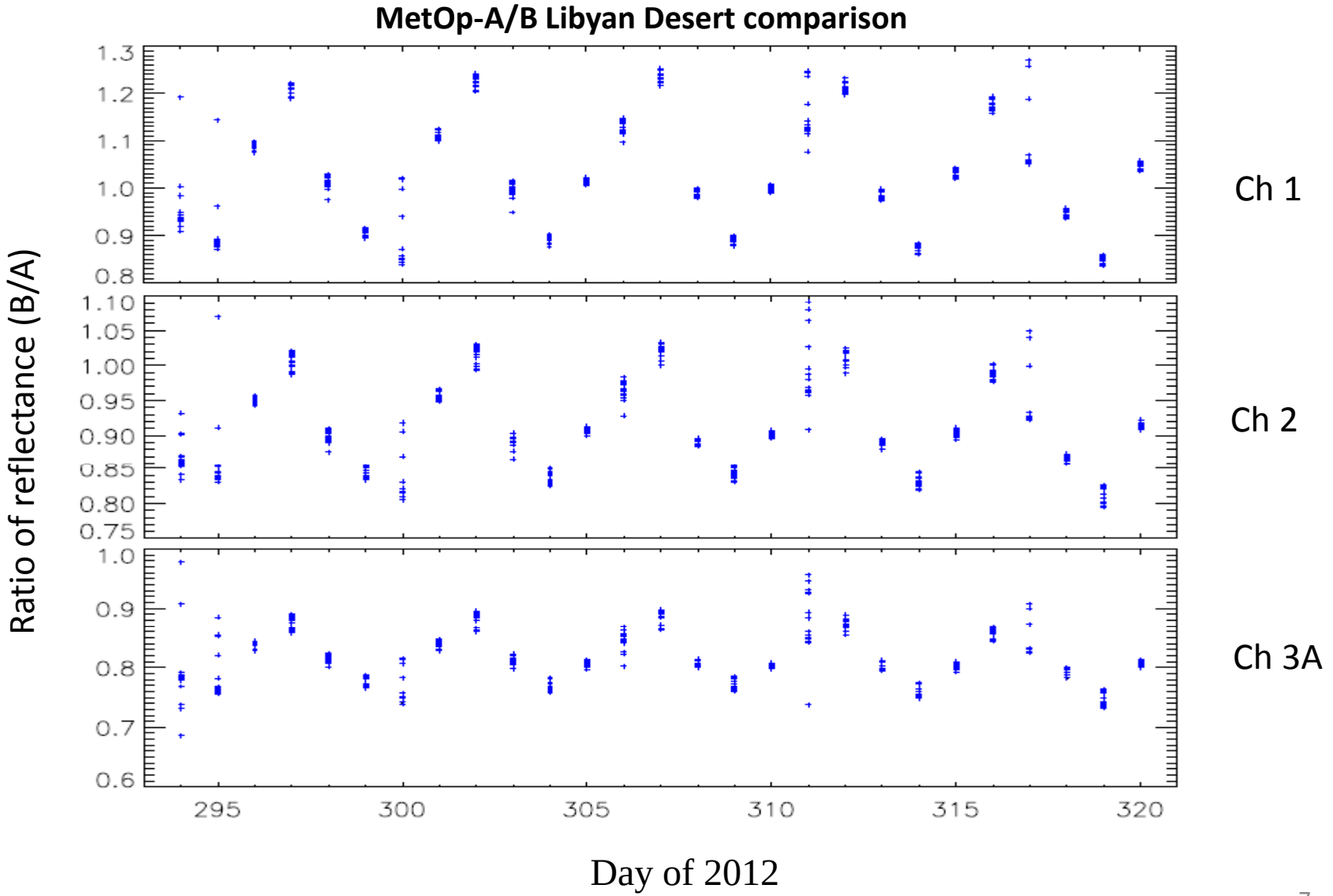

MetOp-A and MetOp-B inter-comparison BRDF effect

+50min

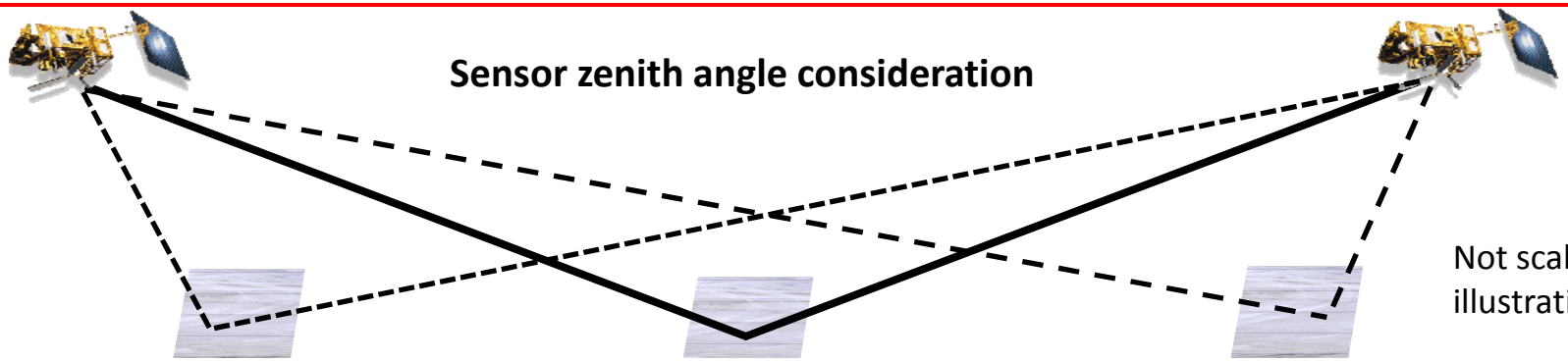

Not scaled for illustration

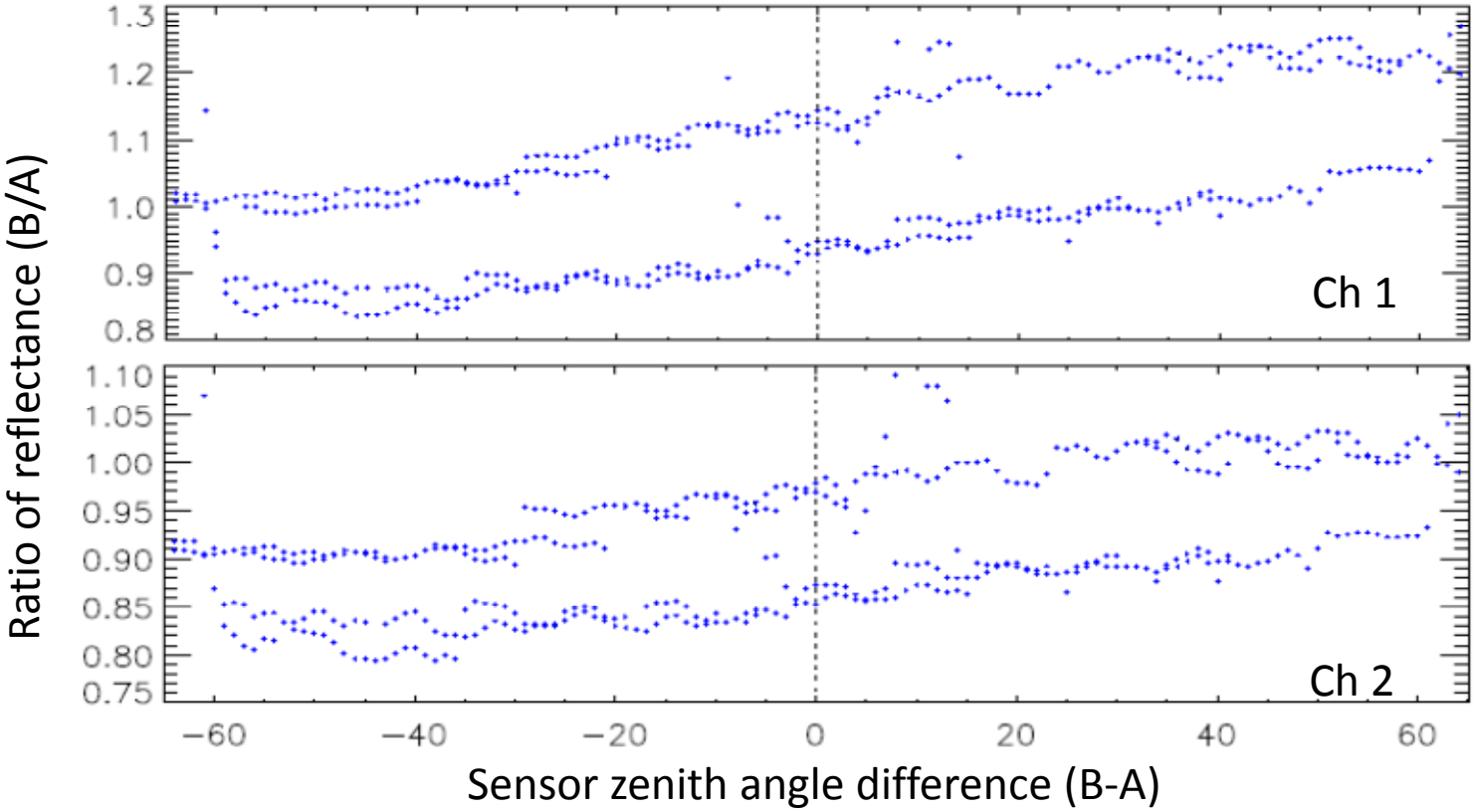

MetOp-A and MetOp-B inter-comparison BRDF effect

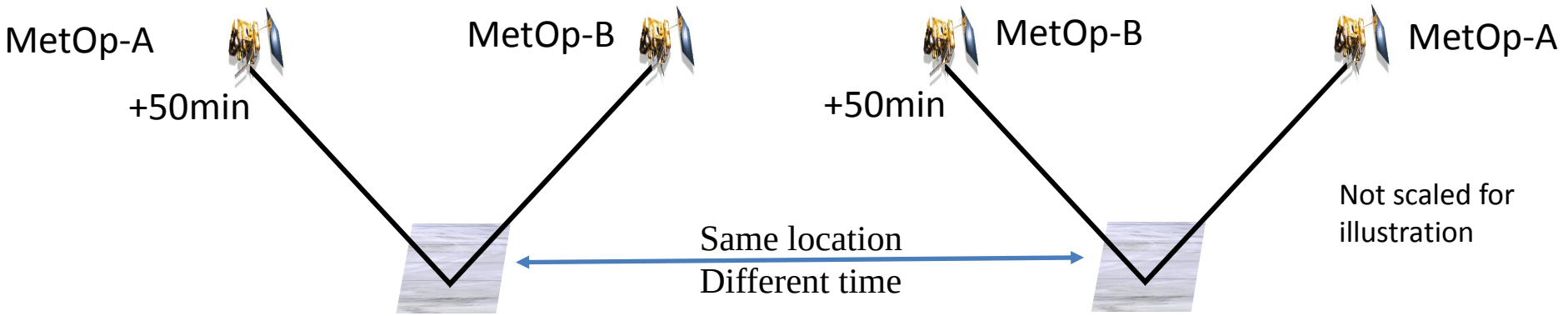

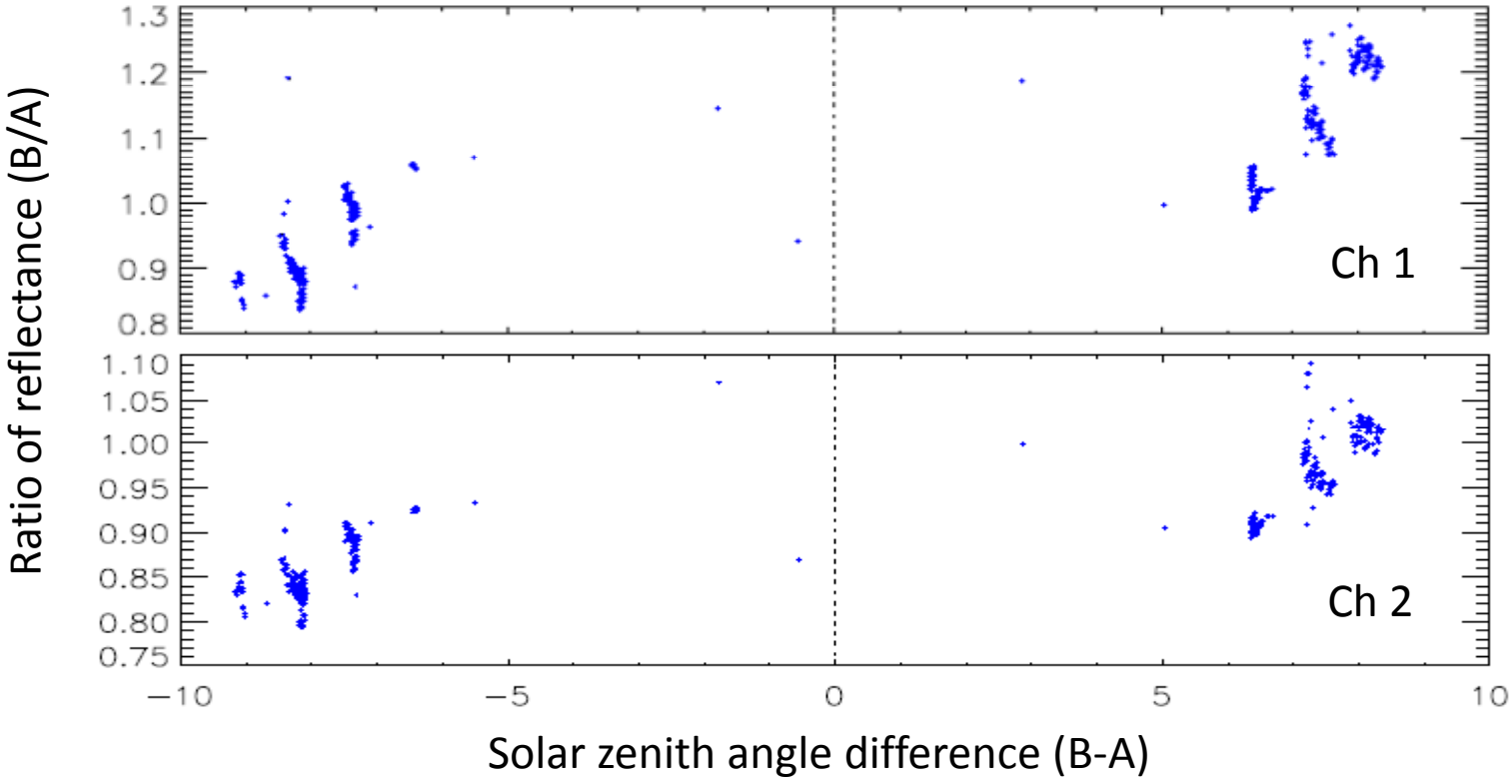

MetOp-A and MetOp-B inter-comparison BRDF effect modeling

Modeling for comparison with zenith angle dependency

$$R_{sensor} = \alpha + p\phi_{sensor\_zenith} + q\phi_{Solar\_zenith}$$

$$\frac{R_B}{R_A} = \frac{\alpha_B + p\phi_{B\_zenith} + q\phi_{Solar\_zenith\_B}}{\alpha + p\phi_{A\_zenith} + q\phi_{Solar\_zenith\_A}}$$

$$= \left(\frac{\alpha_B}{\alpha}\right)\frac{1 + \frac{p\phi_{B\_zenith}}{\alpha_B} + \frac{q\phi_{Solar\_zenith\_B}}{\alpha_B}}{1 + \frac{p\phi_{A\_zenith}}{\alpha} + \frac{q\phi_{Solar\_zenith\_A}}{\alpha}}$$

$$\frac{R_B}{R_A} \approx \left(\frac{\alpha_B}{\alpha}\right) + p'\left(\phi_{B\_zenith} - \phi_{A\_zenith}\right) + q'\left(\phi_{Solar\_zenith\_B} - \phi_{Solar\_zenith\_A}\right)$$

Approximation: 1. $\left(\frac{1}{1+x} \approx 1 - x \quad for\, x << 1\right)$

2. secondary order effect ignored

MetOp-A and MetOp-B inter-comparison with BRDF consideration

Zenith angles consideration

$$\frac{R_B}{R_A} \approx \left(\frac{\alpha_B}{\alpha}\right) + p'\left(\phi_{B\_zenith} - \phi_{A\_zenith}\right) + q'\left(\phi_{Solar\_zenith\_B} - \phi_{Solar\_zenith\_A}\right)$$

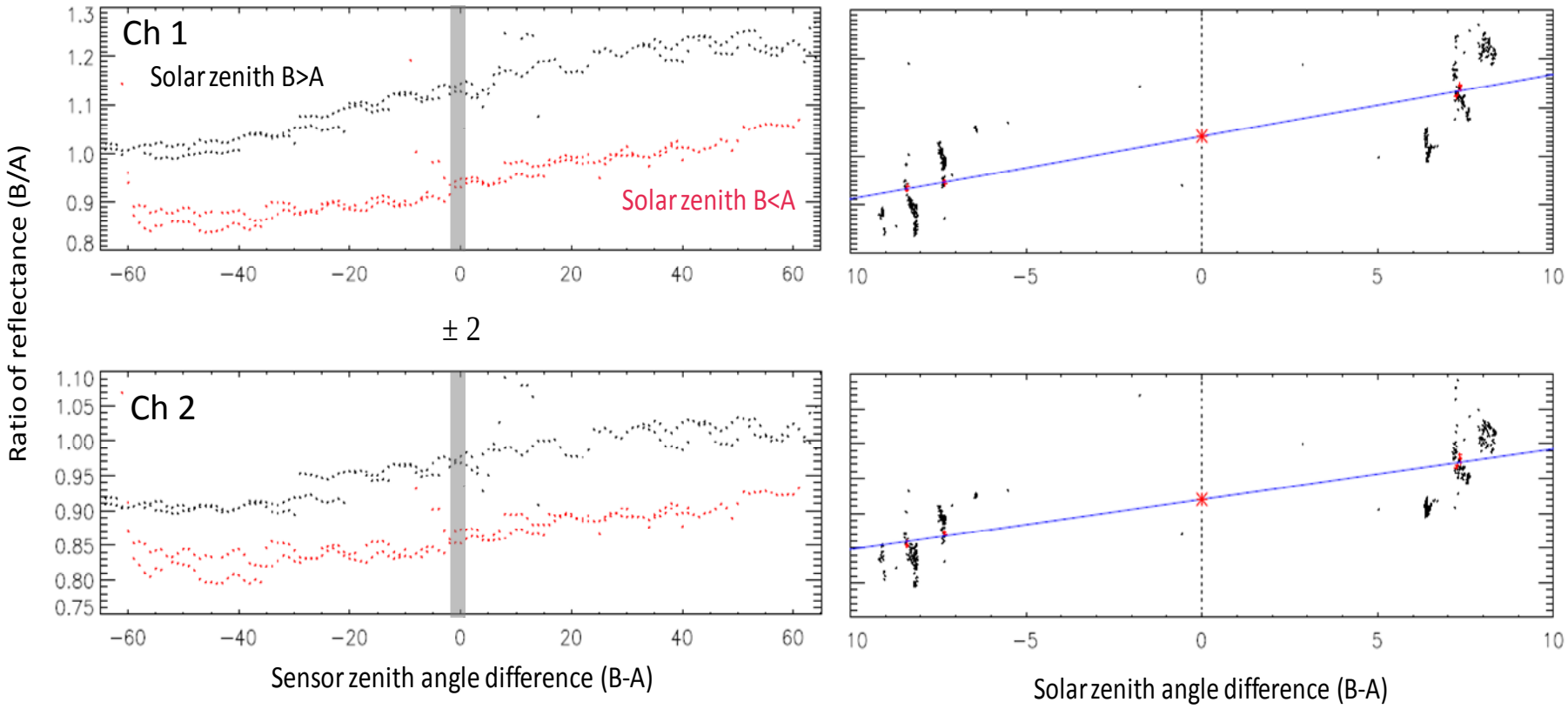

MetOp-A and MetOp-B inter-comparison with BRDF consideration

$$\frac{R_B}{R_A} - p'\left(\phi_{B\_zenith} - \phi_{A\_zenith}\right) \approx \left(\frac{\alpha_B}{\alpha}\right) + q'\left(\phi_{Solar\_zenith\_B} - \phi_{Solar\_zenith\_A}\right)$$

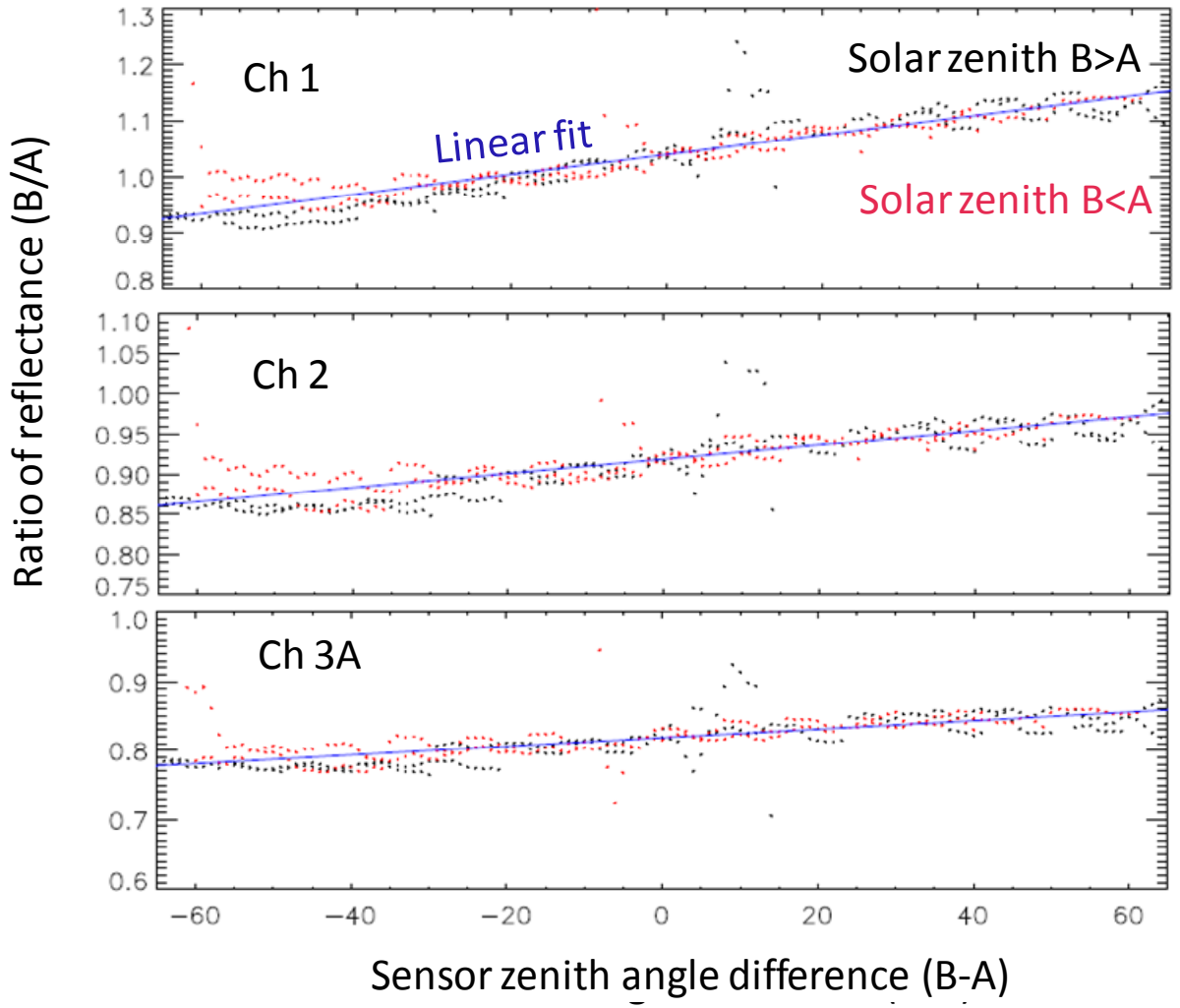

11/15/2012 results using 1 month data

MetOp-A and MetOp-B inter-comparison BRDF modeling results

$$\frac{R_B}{R_A} \approx \left(\frac{\alpha_B}{\alpha}\right) + p'\left(\phi_{B\_zenith} - \phi_{A\_zenith}\right) + q'\left(\phi_{Solar\_zenith\_B} - \phi_{Solar\_zenith\_A}\right)$$

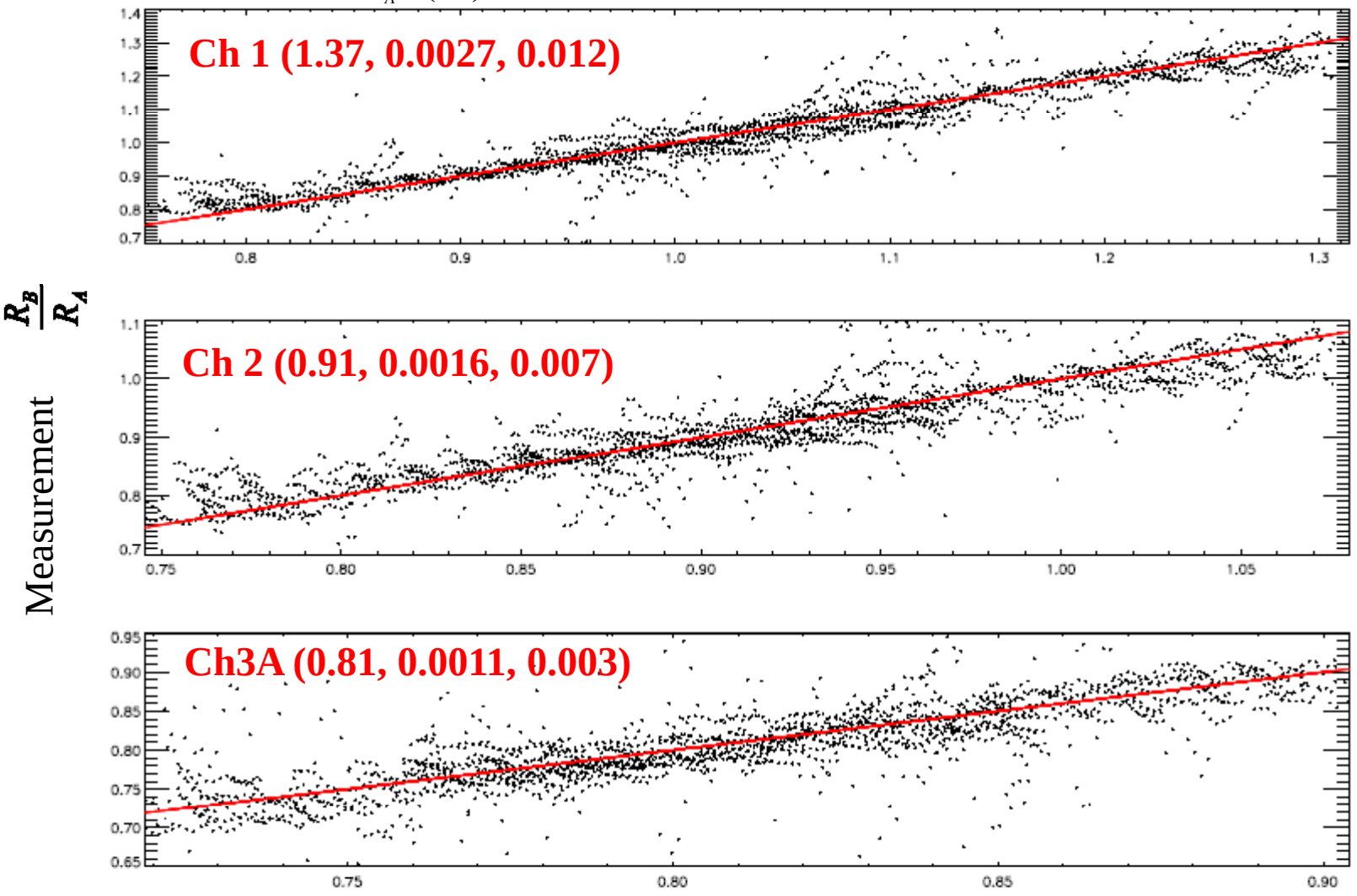

02/26/2012 results using 4 month data

Mode $\left(\frac{\alpha_B}{\alpha}\right) + p'\left(\phi_{B\_zenith} - \phi_{A\_zenith}\right) + q'\left(\phi_{Solar\_zenith\_B} - \phi_{Solar\_zenith\_A}\right)$

AVHRR visible channel calibration using seasonal oscillation

- The modeling of the seasonal oscillation requires data points in certain length of time
- The information from previous AVHRR measurements can be used to predict the seasonal oscillation for MetOp-B AVHRR.
- Assumptions and approaches: The seasonal oscillation phase and amplitude are the same as MetOp-A AVHRR.

NOAA18 data

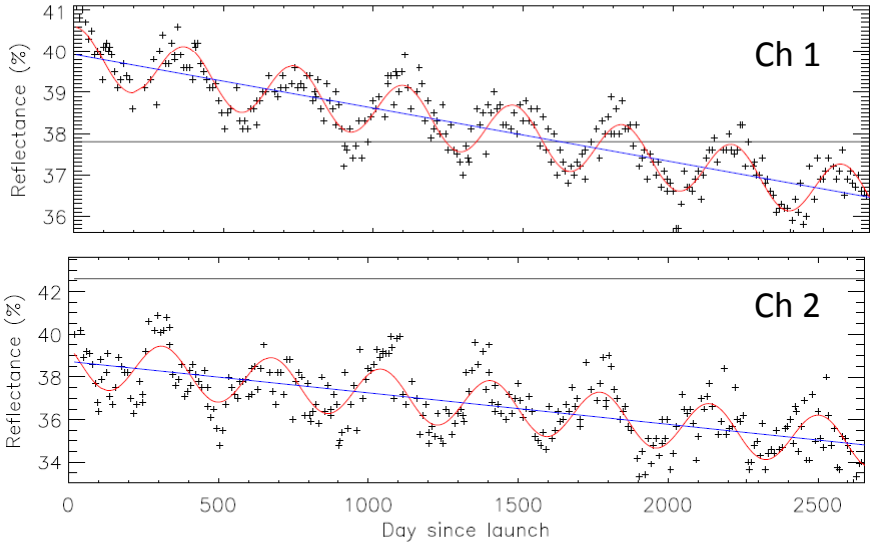

Oscillation derived from NOAA15, 16, 17, 18, 19, and MetOp-A

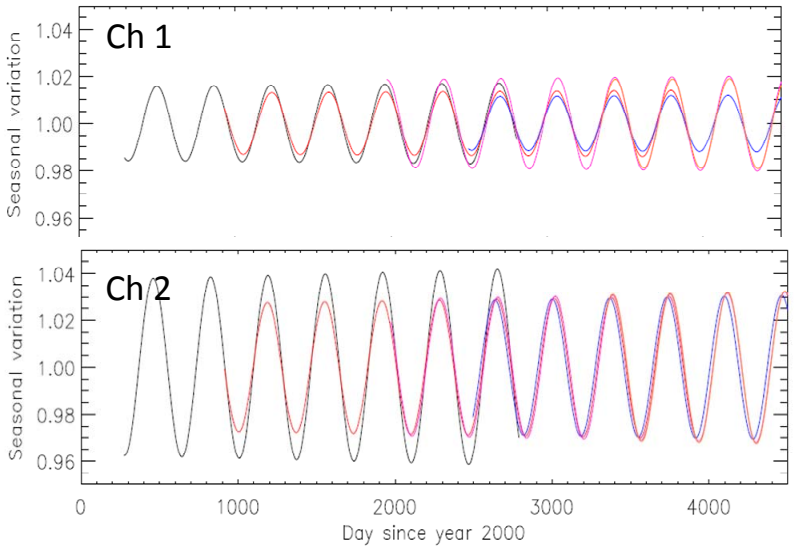

AVHRR visible channel calibration using seasonal oscillation

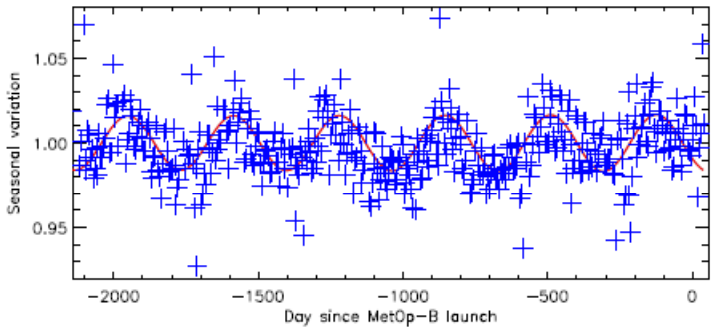

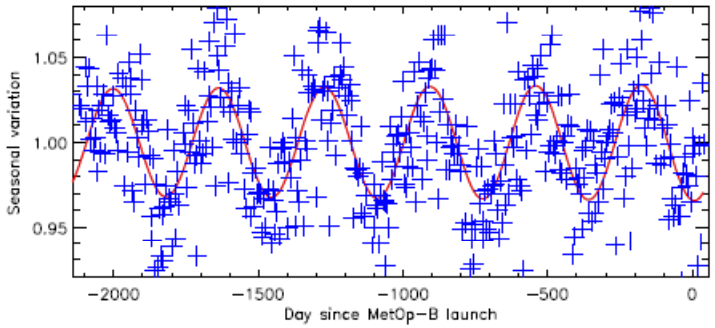

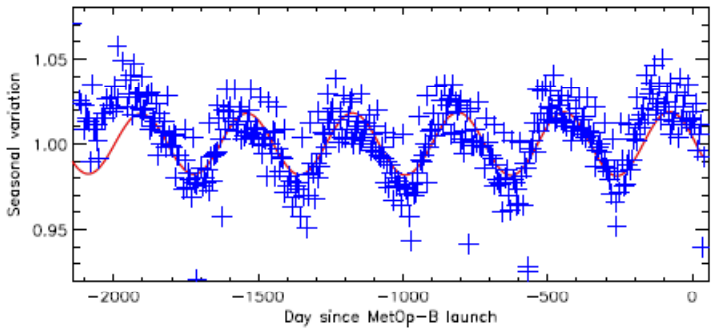

Apply to MetOp-B

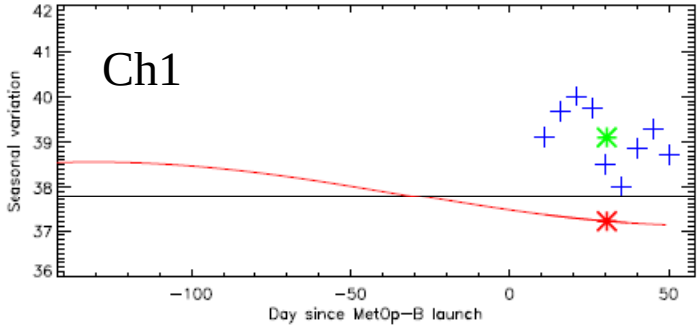

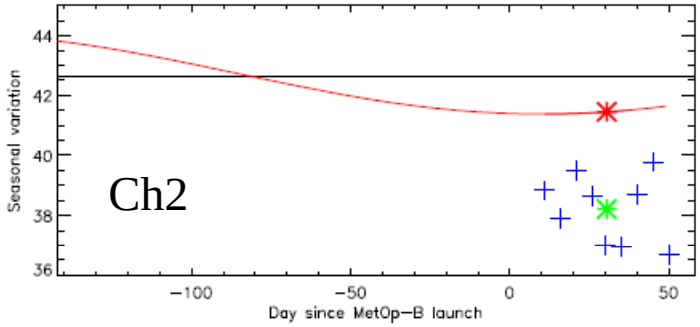

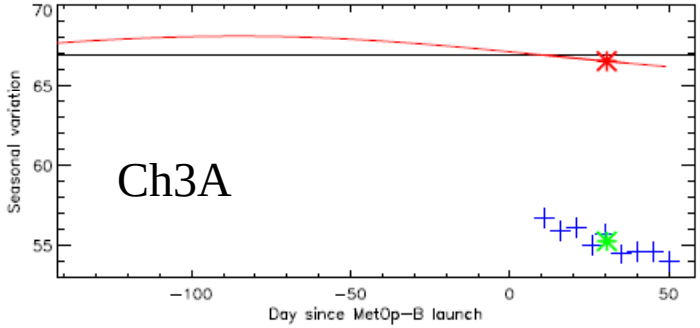

(Left) The seasonal oscillation (red curve) from MetOp-A. The symbols are MetOp-A data corrected by the degradation
(Right) Calibration of MetOp-B with seasonal variation consideration. The red curve is the reference reflectance with seasonal oscillation. The symbols are MetOp-B data

AVHRR visible channel calibration

Calibration updates for channel 1, 2, and 3A.

Update coefficient	Ch 1	Ch 2	Ch3A
Method 1	0.951	1.085	1.205
Method 2	0.961	1.087	1.220
Average	0.956	1.086	1.212

- After the update coefficients derived, The response function (count to albedo conversion) can be updated.
- The black lines from pre-launch calibration. The red lines are the update.
- The accuracy increases with number of the data point.
- The degradation should be considered if the duration of the data is sufficient long.

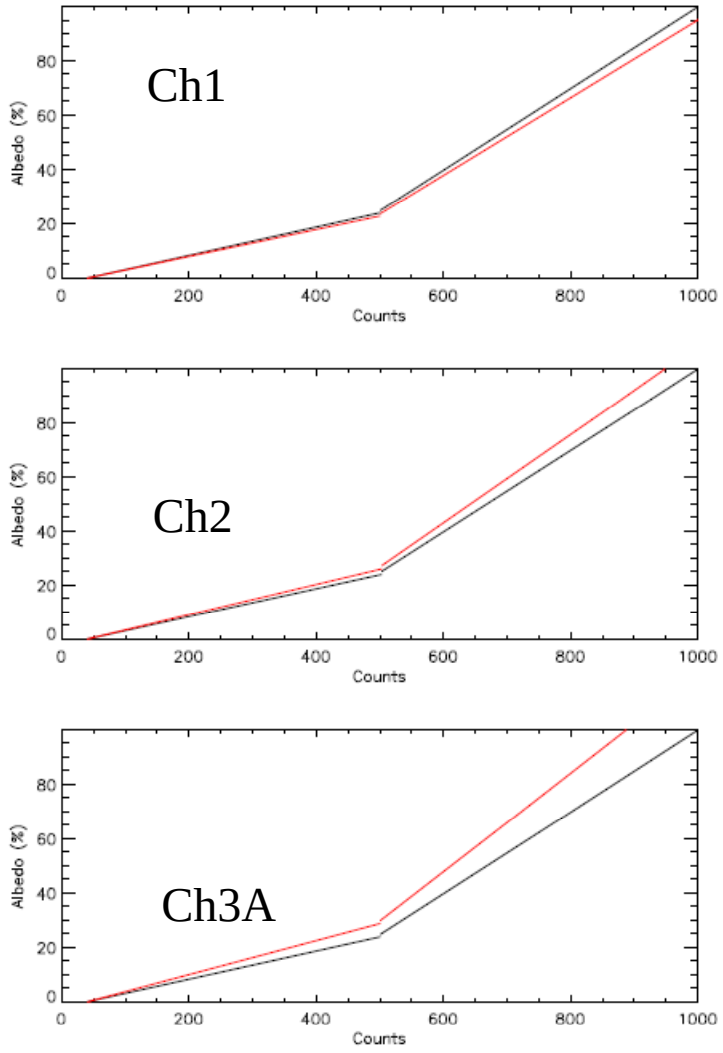

The visible and near-infrared channel response before and after the calibration update. The black lines are from pre-launch calibration and the red lines are on-orbit updated response.

AVHRR visible channel calibration and consistency NDVI verification

Verification of the calibration update using weekly NDVI comparison of MetOp-A and MetOp-B.

Weekly NDVI from MetOp-A/B

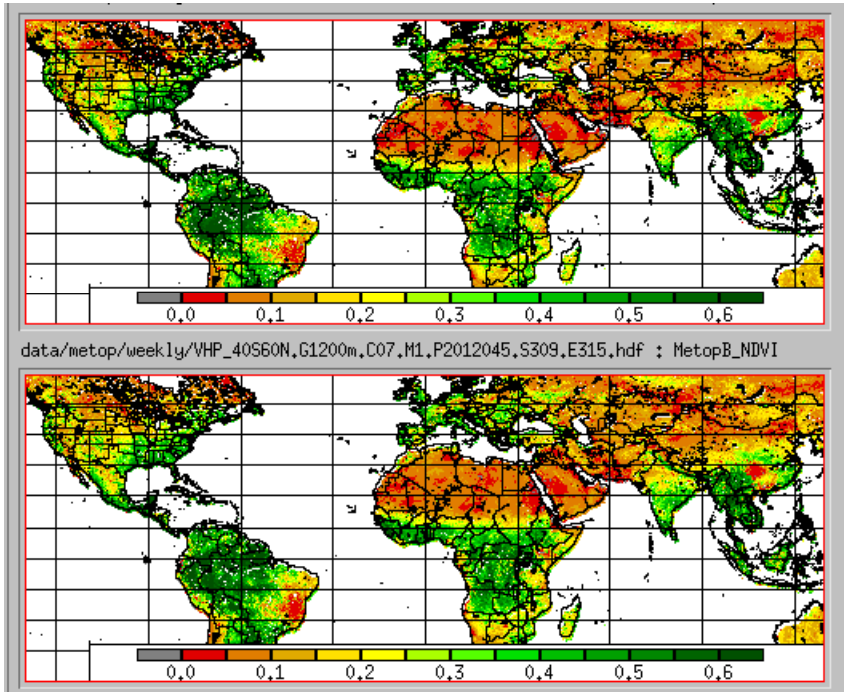

Before and after MetOp-B calibration update

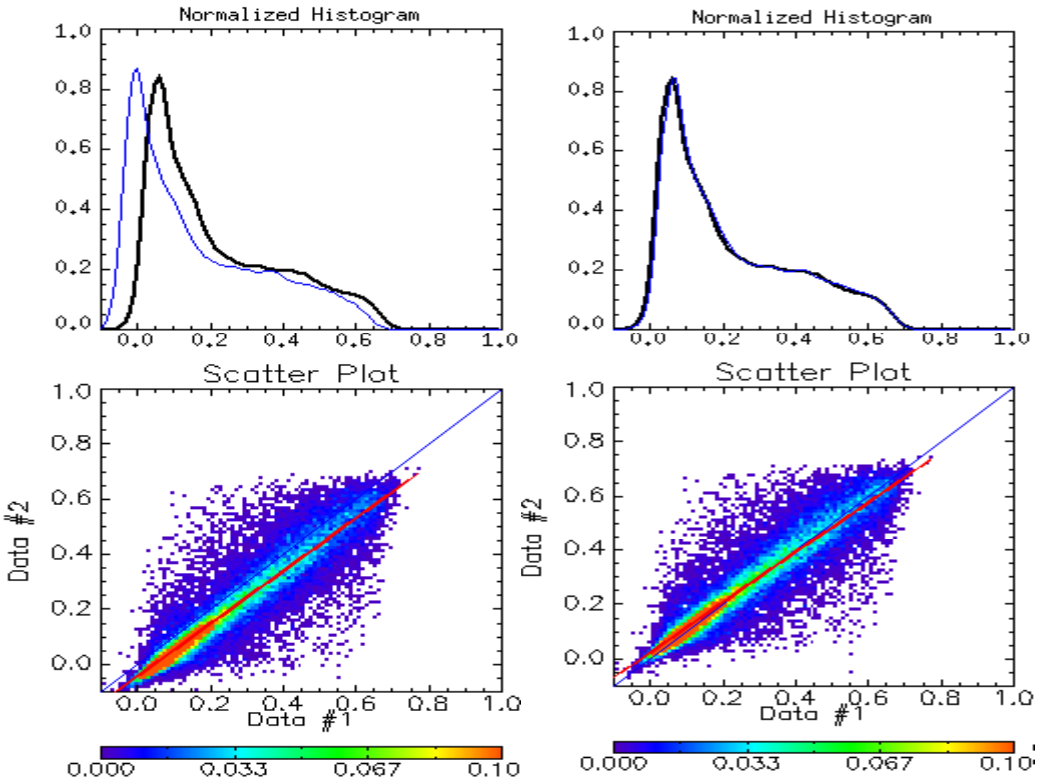

MetOp-A AVHRR Libyan desert seasonal oscillation using curve regression

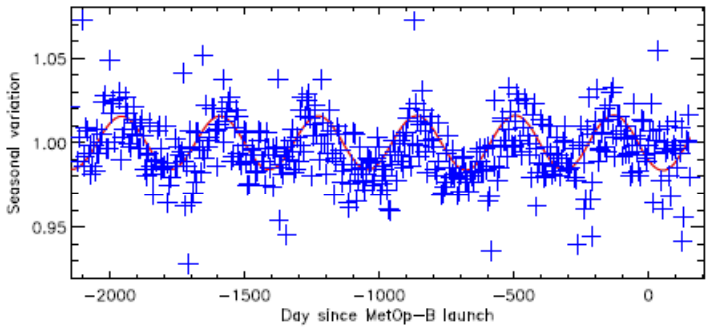

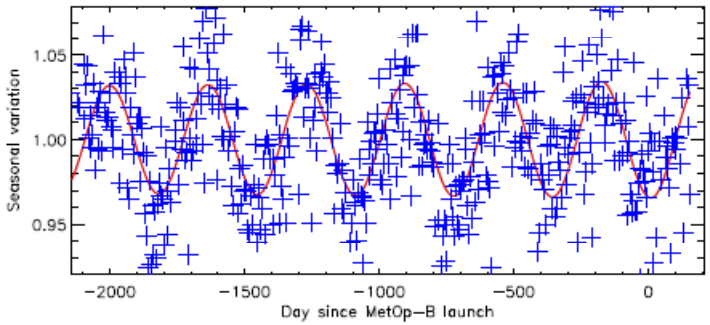

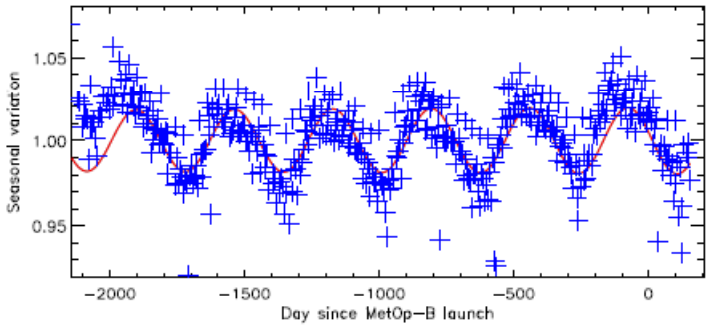

Apply to

MetOp-B

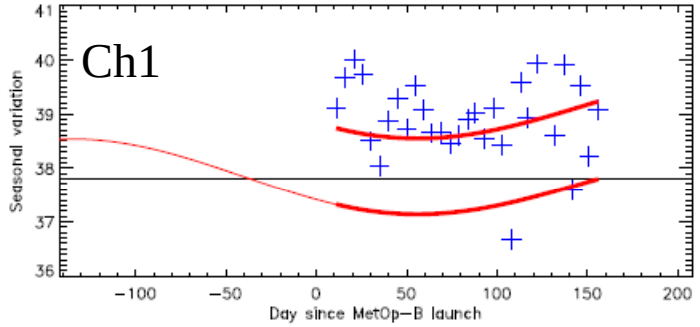

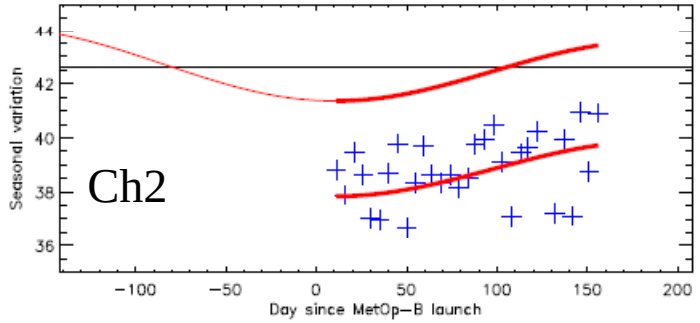

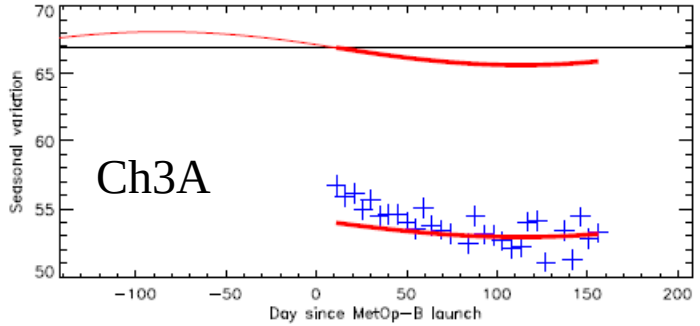

On 02/26/2013, more than 4 month data are used for the calibration update. The seasonal oscillation curve should be considered. An improvement is applied using the regression of the oscillation curve.

Summary

Calibration update calculated 11/15/2012

Update coefficient	Ch 1	Ch 2	Ch3A
Method 1	0.951	1.085	1.205
Method 2	0.961	1.087	1.220
Average	0.956	1.086	1.212

Calibration update calculated 02/26/2013
(Seasonal oscillation curve regression applied)

Update coefficient	Ch 1	Ch 2	Ch3A
Method 1	0.9634	1.0929	1.2400
Method 2	0.9647	1.0939	1.2333
Average	0.964	1.0934	1.2366

Method 1: seasonal oscillation Method 2: BRDF modeling

- Degradation is observed from these two delivery. The degradation in the update is the averaged value over the period of the comparison data used.
- With curve regression of the seasonal oscillation, the results of these two methods are closer.

Summary

- MetOp-A and MetOp-B inter-comparison is performed. The BRDF effect has been modeled and has been considered in the comparison.
- The seasonal oscillation derived from MetOp-A is applied to MetOp-B for calibration update. Applied the curve regression for seasonal oscillation modeling.
- MetOp-B AVHRR visible and near-IR channel calibration update is derivered using these two methods and the calibration update has been verified using NDVI
- The first update was delivered January 2013, and the update now becomes monthly routine task.
- The degradation will be considered in the modeling as longer period of data used. A model will be developed for operational calibration update and for research.